Damping Scaling of Response Spectra for Shallow Crustal Earthquakes in Active Tectonic Regions

S. Rezaeian
U.S. Geological Survey, Golden, CO, USA

Y. Bozorgnia
Pacific Earthquake Engineering Research Center, University of California, Berkeley, CA, USA

I.M. Idriss
University of California, Davis, CA, USA

N. Abrahamson
Pacific Gas & Electric Company, CA, USA

K. Campbell
EQECAT, Inc, Beaverton, OR, USA

W. Silva
Pacific Engineering & Analysis, El Cerrito, CA, USA

ABSTRACT:
Ground motion prediction equations (GMPEs) for elastic response spectra, including the Next Generation Attenuation (NGA) models, are typically developed at a 5% viscous damping ratio. In reality, however, structural and non-structural systems can have damping ratios other than 5%, depending on various factors such as structural types, construction materials, and level of input ground motions. This paper summarizes the findings of a comprehensive study to develop a new model for a Damping Scaling Factor (DSF) that can be used to adjust the 5% damped spectral ordinates predicted by a GMPE for damping ratios between 0.5 to 30%. Using the 2011 version of the NGA-West2 project database of ground motions recorded from worldwide shallow crustal earthquakes in active tectonic regions, dependencies of the DSF on parameters such as spectral period, damping ratio, moment magnitude, source-to-site distance, and duration are examined. The strong influence of duration is captured by inclusion of both magnitude and distance in the DSF model. Influences of other factors such as local site conditions are also examined; however, they do not show significant influence on DSF. The proposed model for DSF provides functional forms for the median value and the logarithmic standard deviation of DSF. The model is developed based on the empirical data of spectral ordinates, and thus, is independent of any specific GMPE. It is also heteroscedastic, where the variance is a function of the damping ratio. The DSF models are developed for the "average" horizontal ground motion components, RotD50 and GMRotI50, as well as the vertical component of ground motion.

Keywords: Damping Scaling Factor, Ground Motion Prediction Equation, Elastic Response Spectra

1. INTRODUCTION

In seismic design, analysis, and hazard calculations of engineered facilities, ground motion prediction equations (GMPEs) are used to predict the intensity of ground shaking. Traditionally, GMPEs are developed for elastic response spectra at a 5% reference damping ratio (e.g., NGA models, see Power et al., 2008). The damping ratio represents the level of energy dissipation in structural, geotechnical, and non-structural systems.

Even though GMPEs are typically developed for a 5% damping ratio, in reality, structures can have damping ratios other than 5%. The value of the damping ratio depends on the structural type, construction material, and level of ground shaking, among other factors. For example, base-isolated structures and structures with added energy dissipation devices can have damping ratios higher than 5%, while some non-structural components can have damping ratios lower than 5%. As another example, the recent guidelines for performance-based seismic design of tall buildings (TBI, 2010) specify a damping ratio of 2.5% for tall buildings at the serviceability hazard level. Generally a lower damping ratio is expected if the structure remains elastic; on the other hand, if the ground shaking is severe enough to cause yielding or damage to the structural and non-structural components, the equivalent damping ratio in a linear analysis could increase significantly. Damping ratios for different types of structures and ground motion levels are a subject of debate, but recommended values and estimation techniques are available in the literature (e.g., Newmark and Hall, 1982; PEER/ATC72-1, 2010; Regulatory Guide 1.61, 2007).

If a system has a damping ratio other than 5%, the predicted 5% damped ground motion intensity should be adjusted to reflect the difference. For example, the classic work of Newmark and Hall (1982), or variations of it, has been used worldwide to scale design spectra for different damping ratios. The pioneering work of Newmark and Hall was based on only 28 records from 9 earthquakes that had occurred prior to 1973. A review of damping scaling rules is provided by Bozorgnia and Campbell (2004) and Naeim and Kircher (2001). In this paper, we use a recently updated NGA database of over 2,000 recordings from shallow crustal earthquakes in active tectonic regions to develop a new model that can be used to scale the 5% spectral ordinates predicted by a GMPE to spectral ordinates for other damping ratios.

In the past two decades, a rather large number of studies have been conducted to obtain response spectral models for damping ratios other than 5%. A comprehensive literature review is provided in Rezaeian et al. (2012). Few studies have developed GMPEs that directly estimate the spectral ordinate at various levels of damping (see details in Rezaeian et al., 2012). This approach requires different GMPE coefficients for different damping ratios. Also, this approach does not facilitate the use of existing GMPEs. An alternative approach that has been taken in the majority of the existing literature and building codes is to develop models for multiplicative factors that scale the 5% damped spectral ordinates predicted by existing GMPEs to ordinates for other damping ratios. We follow the second approach and define the *Damping Scaling Factor* (DSF) as

$$DSF = \frac{Pseudo\ Spectral\ Acceleration\ for\ a\ \beta\%\ damping\ ratio}{Pseudo\ Spectral\ Acceleration\ for\ a\ 5\%\ damping\ ratio} \tag{1.1}$$

where β represents the damping ratio of interest. Various methods in the literature for modeling the DSF can be divided into three categories. The first is methods based on random vibration theory (e.g., procedure recommended by McGuire et al., 2001). The second is methods based on analytical studies that examine the dependence of the *DSF* on various parameters. For example, Cameron and Green (2007) examined the analytical response of a single-degree-of-freedom oscillator to finite-duration, sinusoidal excitations in order to show the dependence of the DSF on the frequency content and the duration of motion. The third is methods based on empirical studies. A comprehensive review of empirical models is presented in Rezaeian et al. (2012). There are significant disagreements among the existing empirical models (see, e.g., Bommer and Mendis, 2005; Lin et al., 2005; Naeim and Kircher, 2001). One should have in mind that different models have used different databases and considered different ranges of the damping ratio and the spectral period which may contribute to the discrepancies. Despite these discrepancies, the majority of the models qualitatively agree on the general trends of the *DSF* with the potential predictor variables.

We empirically develop a predictive equation of the following generic form

$$\ln(DSF) = \mu(\beta, T, earthquake, site; \mathbf{b}) + \epsilon \tag{1.2}$$

where μ represents the mean of $\ln(DSF)$, which is a function of the damping ratio β, the spectral period T, and various earthquake and site characteristics such as earthquake magnitude, source-to-site distance, and soil conditions; $\mathbf{b}$ is the vector of regression coefficients; and ϵ represents the error term that is assumed to be normally distributed with zero mean.

This paper starts by describing the database of strong ground motion records that is used in this study for empirical modeling, followed by a summary of the observed trends between the *DSF* and the potential predictor variables. Next, models for the median *DSF* and its logarithmic standard deviation for the "average" horizontal component are presented. Finally, the extension of the model for the vertical component of ground motion is presented.

2. GROUND MOTION DATABASE

A new database of over 8,000 three-component recordings has been developed for the NGA-West2 project (Ancheta et al., 2012). NGA-West2 is a research program supported by the Pacific Earthquake Engineering Research Center (PEER) to update the 2008 Next Generation Attenuation (NGA) GMPEs for shallow crustal earthquakes in active tectonic regions. In this database, the elastic response spectra for the horizontal and vertical components have been calculated for 11 damping ratios: $\beta = 0.5$, 1, 2, 3, 5, 7, 10, 15, 20, 25, and 30%.

The "horizontal" components in the NGA database include "as-recorded" horizontal motions, GMRotI50 horizontal component (Boore et al., 2006), and RotD50 horizontal component (Boore, 2010). The last two are representative of the "average" horizontal ground motion and are independent of the in-situ orientation of a seismometer. We developed *DSF* models for GMRotI50, RotD50, and vertical components. This paper presents the results for the RotD50 (i.e., horizontal) and the vertical components. The results for the GMRotI50 component can be found in Rezaeian et al. (2012).

We used the 2011 version of the NGA-West2 database. To ensure a proper damping scaling for near-source data, we selected the records with closest distance to rupture, R_{rup}, of less than 50km. This subset contains 2,250 records for the horizontal components and 2,229 records for the vertical component. The moment magnitude, **M**, ranges between 4.2 to 7.9. The magnitude-distance distribution of the selected records is shown in Fig. 2.1. The validity of the developed model is later verified for distances beyond 50km by examining the residual plots of the corresponding records.

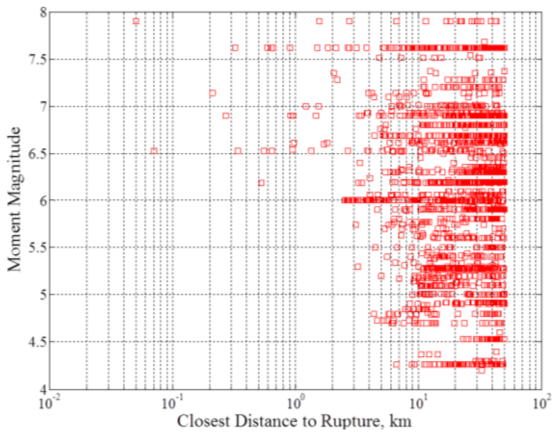

Figure 2.1. Magnitude-distance distribution of the selected database (horizontal component).

To measure ground motion duration, we use D_{5-75}, the significant duration of motion from 5-75% of Arias intensity. This measure is calculated for each record in the database to examine the expected dependence of the *DSF* on the duration of the motion. For the horizontal component, we take the arithmetic average of D_{5-75} for the two "as-recorded" horizontal components.

The *DSF* is calculated according to Eqn. 1.1 for each record in the database at all 11 damping ratios and at 21 spectral periods: $T = 0.01$, 0.02, 0.03, 0.05, 0.075, 0.1, 0.15, 0.2, 0.25, 0.3, 0.4, 0.5, 0.75, 1, 1.5, 2, 3, 4, 5, 7.5, and 10s.

3. PREDICTOR VARIABLES

To identify the predictor variables in Eqn. 1.2, we extract patterns and examine the dependence of the DSF on various variables in our database. We start with the variables identified in the literature to possibly have influence on the DSF. These variables include: the damping ratio β, which is a common predictor variable in all existing empirical models; the spectral period T, which is considered in the majority of existing models; duration, magnitude, and distance, which have been the subject of interest in more recent studies; and site conditions, which have been considered in very few studies.

The most fundamental predictor variables for the DSF are β and T. While the dependence of the DSF on these two variables is apparent theoretically, different degrees of dependence have been reported in the literature. For example, mild, weak and very weak dependence on T has been reported by Stafford et al. (2008), Bommer and Mendis (2005), and Naeim and Kircher (2001), respectively. Statistical analysis of our database reveals systematic patterns between DSF and these two variables as seen in Fig. 3.1. There is almost no dependence on T between 0.2 - 2s for $\beta \geq 2\%$, but there is a strong dependence outside this period range until the DSF approaches unity for very short and very long T. This is expected because the forces in a very stiff or a very flexible structure are relatively independent of the damping ratio. The dependence on T is much stronger for $\beta \leq 1\%$.

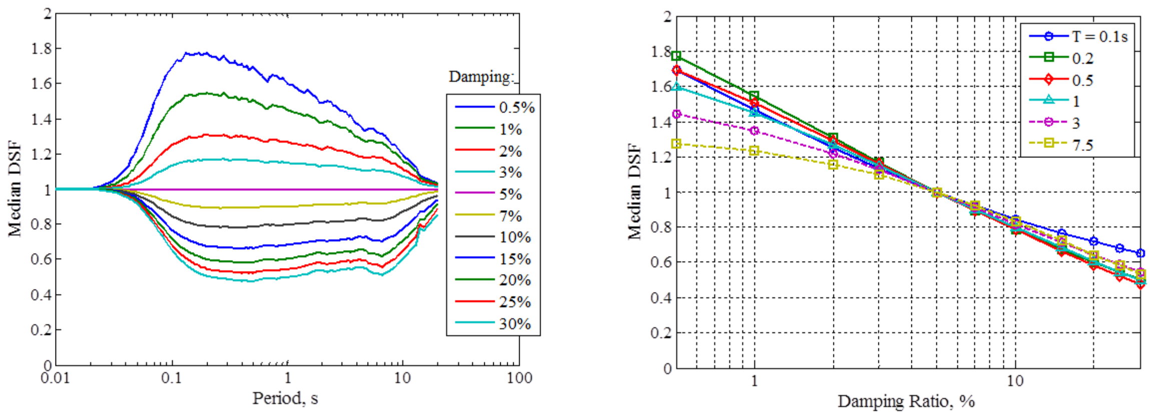

(a) **(b)**

Figure 3.1. Influence of spectral period and damping ratio on DSF.

Duration of the ground motion can be an important factor controlling the DSF, as the number of energy dissipating cycles can be influential. The influence of duration on the DSF is also acknowledged by Stafford et al. (2008), Cameron and Green (2007), and Bommer and Mendis (2005). Our data show an increase in DSF with D_{5-75} for $\beta < 5\%$, and a decrease for $\beta > 5\%$. Fig. 3.2 shows the data at $T = 1$s along with a fitted line to indicate the linear correlation between DSF and $\log(D_{5-75})$ for visual purposes. The dependence of the DSF on duration becomes stronger as T increases and as β deviates from 5%.

Explicit inclusion of duration in the model is not ideal in practice because duration is generally not specified as part of a seismic design scenario. In general, there is a strong positive correlation between duration and earthquake magnitude and a moderate positive correlation between duration and distance (e.g., Kempton and Stewart, 2006). Therefore, we consider whether the influence of duration on the DSF can be captured by including magnitude and distance in our model. Our data show a strong dependence between DSF and **M**. An example is shown in Fig. 3.3 at $T = 1$s along with a fitted line to show the linear correlation in the trends. Similar to D_{5-75}, the dependence on **M** is more pronounced at longer T and as β deviates from 5%. Similar patterns, but far less significant, are seen between DSF and R_{rup} (see Fig. 3.4). By performing regression analysis and scrutinizing the residual diagnostic plots, we find that most of the influence of duration on the DSF can be captured through inclusion of **M** in the model. Furthermore, we find that despite the weak influence of distance, some of the residual effects of duration left after including **M** can be captured by including R_{rup} in the model.

Influences of site conditions and tectonic setting have been considered in the literature. Our focus is on shallow crustal events in active tectonic regions; thus, we do not consider the tectonic setting as a predictor variable. To consider the effect of site conditions, we examine the influence of V_{S30} (time-averaged shear-wave velocity in the top 30m of the site) on DSF. An insignificant dependence is observed, which is consistent with the literature. For example, Bommer and Mendis (2005) reported that soft soil influences the DSF but to a much lesser degree than magnitude and distance. Lin and Chang (2004) included site class in their model, but they report that this factor can be neglected when the DSF is calculated for the pseudo-spectral acceleration (i.e., Eqn. 1.1). Therefore, we do not consider V_{S30} as a predictor variable.

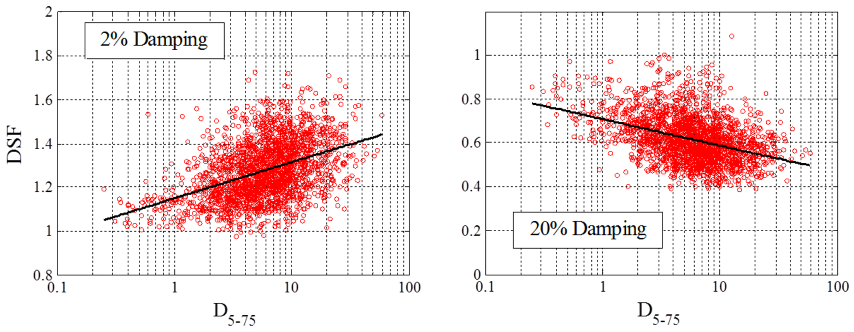

Figure 3.2. Influence of duration on DSF at $T = 1$s.

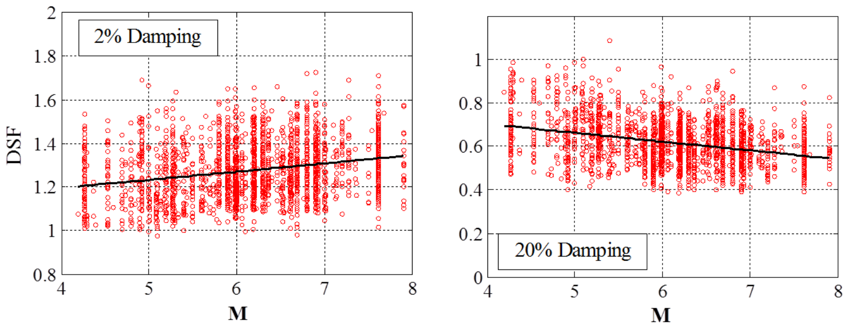

Figure 3.3. Influence of magnitude on DSF at $T = 1$s.

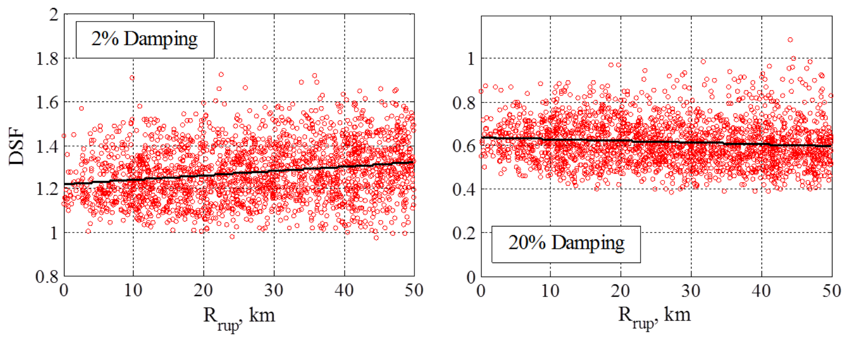

Figure 3.4. Influence of distance on DSF at $T = 1$s.

4. MODEL DEVELOPEMENT

The predictor variables included in the model are selected as described in the previous section. After scrutinizing the data and performing statistical analyses, a lognormal distribution is assigned to the random variable DSF. The functional form for the mean of $\ln(DSF)$ is selected by examining the observed trends between DSF and the predictor variables in our database, as well as by reviewing various functions used in the literature. Regression analysis is then performed to estimate the model coefficients and the variance using the selected database of records with $R_{rup} < 50$km.

To arrive at the final form of the model for median DSF, we follow a step-by-step model building process, details of which are given in Rezaeian et al. (2012). At each combination of the 21 specified periods and the 11 selected damping ratios, we regress DSF on various functions of the predictor variables $\mathbf{M}$ and R_{rup}. Each term is added to the model one at a time, and the residuals versus **M**, R_{rup}, and D_{5-75} are examined. In our view, a linear magnitude term is necessary and sufficient to capture the dependence of data on **M** and most of the dependence on D_{5-75}. The addition of a logarithmic function of R_{rup} further reduces (although not as much as the magnitude term) the dependence on D_{5-75}. It is convenient to directly include β as a predictor variable in the model. To achieve this goal, the dependences of the constant term, the coefficient of the magnitude term, and the coefficient of the distance term, on β are examined. This dependence is captured best by a quadratic function of $\ln(\beta)$. The resulting model is validated by examining the scatter plots of the residuals (i.e., the difference between the observed values of DSF and the model) versus the predictor variables β, **M**, and R_{rup}, and versus other parameters such as D_{5-75}, D_{5-95}, V_{S30}, and sediment depth (i.e., $Z_{1.0}$ and $Z_{2.5}$, respectively representing the depth to the 1.0 and 2.5 km/s shear-wave velocity horizons). The results show that the residuals are symmetrically scattered above and below the zero level with no obvious systematic trends.

4.1. The proposed model for median *DSF*

The final model has the following functional form

$$\ln(DSF) = \begin{array}{l} b_0 + b_1\ln(\beta) + b_2(\ln(\beta))^2 \\ +[b_3 + b_4\ln(\beta) + b_5(\ln(\beta))^2\,]\mathbf{M} \\ +[b_6 + b_7\ln(\beta) + b_8(\ln(\beta))^2\,]\ln(R_{rup}+1) \\ +\,\epsilon \end{array} \tag{4.1}$$

where β is the damping ratio in percentage (e.g., $\beta = 2$ for 2% damping); R_{rup} is in km; b_i, $i = 0, \ldots, 8$, are the period-dependent regression coefficients listed in Table 4.1 for the RotD50 horizontal component; and ϵ is a zero-mean normally distributed random variable with standard deviation σ. A model for σ is presented in the next section. The regression coefficients for the GMRotI50 component are provided in Rezaeian et al. (2012). Minor differences are seen between the models for RotD50 and GMRotI50. Fig. 4.1 shows the predicted DSF values according to Eqn. 4.1 for $\mathbf{M} = 7$ and $R_{rup} = 10$km. As an example, the damping scaling factor is applied to the geometric mean of the five NGA GMPEs and is plotted versus period in Fig. 4.2.

4.2. The proposed model for standard deviation

The standard deviation σ in Eqn. 4.1 is calculated for all combinations of T and β. The data suggest dependence of the variance on the damping ratio. As expected, the standard deviation is zero at 5% damping ($DSF = 1$ for $\beta = 5\%$) and it increases as the damping ratio deviates from 5% reaching a maximum of about 0.2 (see Fig. 4.3.a). This dependence, at a specified period, can be captured by the following equation:

$$\sigma_{\ln(DSF)} = \left| a_0 \ln\left(\frac{\beta}{5}\right) + a_1\left(\ln\left(\frac{\beta}{5}\right)\right)^2 \right| \tag{4.2}$$

where a_0 and a_1 are obtained by fitting (using least squares regression) Eqn. 4.2 to the data from 11 damping ratios. Their values are given in Table 4.1 for the RotD50 component. The predicted standard deviation according to Eqn. 4.2 is plotted in Fig. 4.3.b.

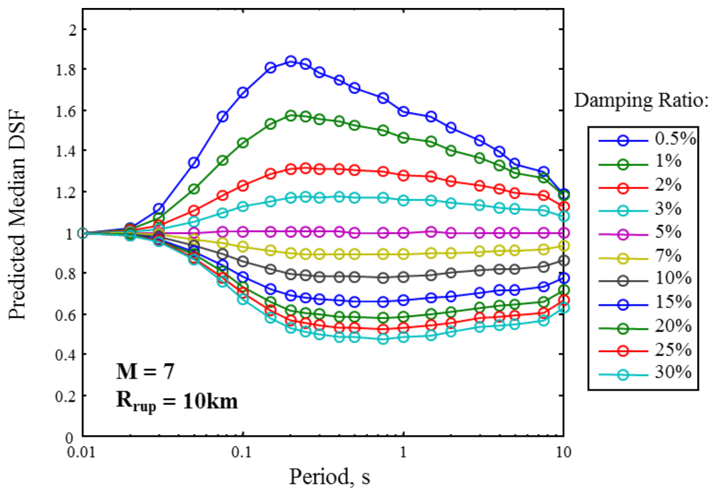

Figure 4.1. Predicted median DSF according to Eqn. 4.1 for the RotD50 component.

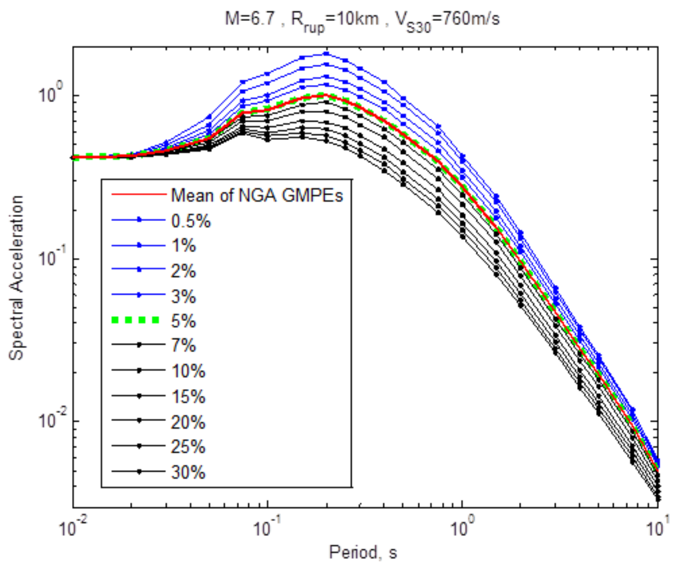

Figure 4.2. The geometric mean of the five NGA GMPEs (red) is scaled to adjust for various damping ratios from 0.5 to 30%. The DSF model for the RotD50 component is used. Assumptions: reverse fault, dip = 45°, hanging wall, fault rupture width = 15km, $R_{jb} = 0$km, $R_x = 7$km.

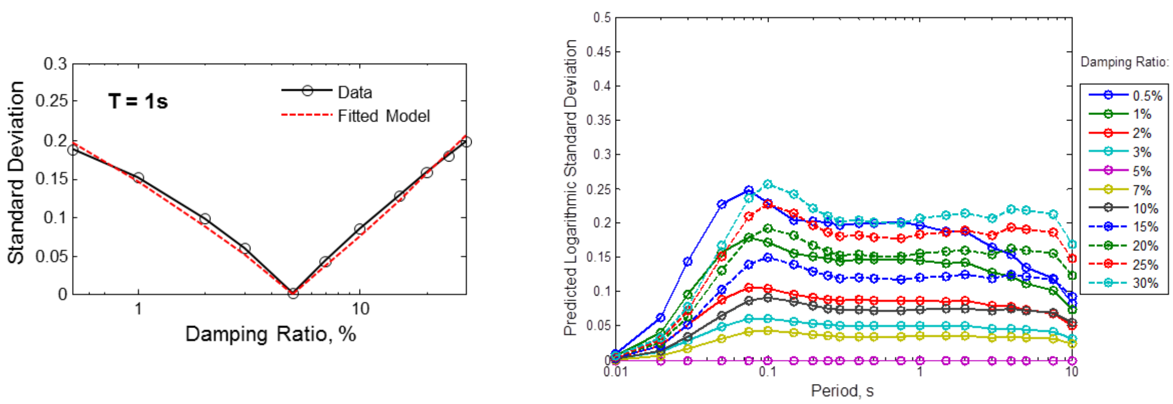

(a) **(b)**

Figure 4.3. (a) Dependence of standard deviation on $\boldsymbol{\beta}$ and the fitted function according to Eqn. 4.2. **(b)** Predicted logarithmic standard deviation according to Eqn. 4.2.

Table 4.1. Regression coefficients for the horizontal component RotD50.

T, s	b_0	b_1	b_2	b_3	b_4	b_5	b_6	b_7	b_8	a_0	a_1
0.01	1.73E-03	-2.07E-04	-6.29E-04	1.08E-06	-8.24E-05	7.36E-05	-1.07E-03	9.08E-04	-2.02E-04	-3.70E-03	2.30E-04
0.02	5.53E-02	-3.77E-02	2.15E-03	-4.30E-03	3.21E-03	-3.32E-04	-4.75E-03	2.52E-03	2.29E-04	-2.19E-02	2.11E-03
0.03	1.22E-01	-7.02E-02	-2.28E-03	-3.21E-03	6.91E-05	9.82E-04	-1.30E-02	7.82E-03	2.27E-04	-5.21E-02	4.60E-03
0.05	2.39E-01	-1.06E-01	-2.63E-02	-8.57E-04	-7.43E-03	4.87E-03	-1.69E-02	8.08E-03	1.71E-03	-9.57E-02	1.31E-03
0.075	3.05E-01	-7.32E-02	-7.29E-02	2.02E-04	-1.64E-02	1.03E-02	-9.26E-04	-6.40E-03	4.42E-03	-1.21E-01	-5.79E-03
0.1	2.69E-01	4.18E-03	-1.07E-01	5.80E-03	-2.49E-02	1.34E-02	2.35E-02	-2.37E-02	5.84E-03	-1.24E-01	-1.08E-02
0.15	1.41E-01	1.00E-01	-1.18E-01	3.01E-02	-4.09E-02	1.41E-02	3.16E-02	-2.47E-02	3.15E-03	-1.15E-01	-1.14E-02
0.2	5.01E-02	1.45E-01	-1.11E-01	4.69E-02	-4.77E-02	1.18E-02	3.10E-02	-2.29E-02	2.41E-03	-1.08E-01	-8.85E-03
0.25	2.28E-02	1.43E-01	-9.73E-02	5.20E-02	-4.70E-02	9.47E-03	2.71E-02	-2.02E-02	1.31E-03	-1.04E-01	-7.35E-03
0.3	-1.58E-02	1.48E-01	-8.83E-02	5.21E-02	-4.36E-02	7.33E-03	3.87E-02	-2.66E-02	1.76E-03	-1.01E-01	-6.90E-03
0.4	2.24E-02	1.03E-01	-7.41E-02	4.63E-02	-3.58E-02	4.65E-03	3.63E-02	-2.45E-02	1.18E-03	-1.02E-01	-6.71E-03
0.5	3.19E-02	7.04E-02	-5.57E-02	4.25E-02	-2.94E-02	1.88E-03	3.87E-02	-2.47E-02	3.13E-04	-1.01E-01	-6.22E-03
0.75	1.04E-02	5.33E-02	-3.72E-02	4.47E-02	-2.40E-02	-2.40E-03	3.47E-02	-2.59E-02	2.90E-03	-1.01E-01	-5.86E-03
1	-8.84E-02	8.92E-02	-2.14E-02	4.98E-02	-2.36E-02	-4.70E-03	5.02E-02	-3.43E-02	2.32E-03	-1.02E-01	-7.31E-03
1.5	-1.57E-01	9.33E-02	3.28E-03	5.85E-02	-2.36E-02	-8.02E-03	4.81E-02	-3.30E-02	2.10E-03	-1.02E-01	-8.75E-03
2	-2.96E-01	1.50E-01	2.09E-02	7.30E-02	-2.96E-02	-9.95E-03	5.24E-02	-3.32E-02	6.86E-04	-1.03E-01	-9.22E-03
3	-4.07E-01	1.97E-01	3.28E-02	8.35E-02	-3.54E-02	-1.01E-02	5.57E-02	-2.91E-02	-3.17E-03	-9.63E-02	-1.07E-02
4	-4.49E-01	2.07E-01	4.42E-02	8.75E-02	-3.59E-02	-1.14E-02	5.07E-02	-2.43E-02	-4.67E-03	-9.83E-02	-1.37E-02
5	-4.98E-01	2.17E-01	5.36E-02	9.03E-02	-3.48E-02	-1.29E-02	5.19E-02	-2.30E-02	-5.68E-03	-9.42E-02	-1.53E-02
7.5	-5.25E-01	2.06E-01	7.79E-02	9.88E-02	-3.76E-02	-1.51E-02	2.91E-02	-4.93E-03	-9.02E-03	-8.95E-02	-1.63E-02
10	-3.89E-01	1.43E-01	6.12E-02	7.14E-02	-2.36E-02	-1.30E-02	2.33E-02	-5.46E-03	-5.92E-03	-6.89E-02	-1.43E-02

As previously mentioned, the regression is performed using data with $R_{rup} < 50$km. The applicability of the model for longer distances is investigated by studying the residual diagnostic plots for records with $R_{rup} \geq 50$km. We conclude that our proposed model can be used for distances of up to 200km without any modifications. We compare our final model with computed DSF values from the database of recorded ground motions and with selected existing models. These comparisons are presented in Rezaeian et al. (2012). As anticipated, we observe close agreement between the model and the data.

5. DAMPING SCALING MODEL FOR VERTICAL COMPONENT

We calculate the DSF for vertical component of ground motions in our database. The dependencies we observe between the vertical DSF and the predictor variables discussed in Section 3 are similar to our observations for the horizontal component. We follow the same approach of the step-by-step regression and study of residual diagnostic plots that was described in Section 4. The functional forms for the vertical DSF model are the same as Eqns. 4.1 and 4.2. The regression coefficients, however, are different and can be found in Rezaeian et al. (2012). In general, the peak of the median DSF for the vertical component is shifted towards shorter periods and is more extreme compared to that for the horizontal component. The most significant differences from the horizontal DSF are seen at $T \leq 0.2$s. Fig. 5.1.a shows the vertical and horizontal DSF at $\mathbf{M} = 7$ and $R_{rup} = 10$km. The standard deviation for the vertical DSF is in general a little higher than that for the horizontal component. It varies between 0 and 0.3. Fig. 5.1.b plots the standard deviation versus period at different damping ratios. We suspect this effect is due to the "averaging" of the two horizontal components, which is expected to reduce the standard deviation compared to the one component used for the vertical ground motion.

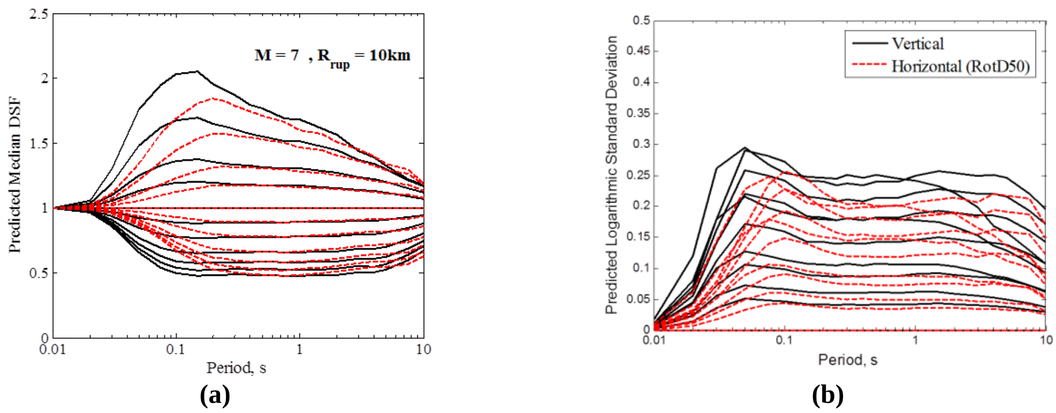

Figure 5.1. Comparisons of predicted **(a)** median and **(b)** logarithmic standard deviation for the vertical versus horizontal DSF.

6. CONCLUSIONS

This paper summarizes the findings of a comprehensive study on the development of damping scaling factors (DSF) for horizontal and vertical ground motions. This study develops a new model for the DSF, which can be used to scale pseudo-spectral acceleration (PSA) values predicted at a 5% damping ratio to PSA values at damping ratios other than 5%. We selected a subset of a very comprehensive update of the NGA ground motion database of recorded ground motions from shallow crustal earthquakes in active tectonic regions. Our selected database includes over 2,000 recordings. In addition to the damping ratio and the spectral period, the predictor variables in our model are magnitude and distance. By including these two variables in the model, we also capture the effect of the duration of motion on the DSF. The final model for the median DSF and its logarithmic standard deviation are presented in Eqns. 4.1 and 4.2. The period-dependent regression coefficients are calculated for the "average" horizontal and the vertical components of ground motion. The proposed model is applicable for periods ranging between 0.01 to 10s, damping ratios from 0.5 to 30%, moment magnitudes between 4.5 and 8.0, and distances of less than 200km.

AKCNOWLEDGMENT
This study was sponsored by the Pacific Earthquake Engineering Research Center (PEER) and funded by the California Earthquake Authority, California Department of Transportation, and the Pacific Gas & Electric Company. Any opinions, findings, and conclusions or recommendations expressed in this material are those of the authors and do not necessarily reflect those of the above mentioned agencies, but do represent the view of the U.S. Geological Survey. We would like to thank all the NGA model developers and supporting researchers for their assistance and valuable feedback throughout this project. Efforts and cooperation of Dr. Tim Ancheta are gratefully acknowledged.

REFERENCES

Ancheta, T., Darragh, R., Silva, W., Abrahamson, N., Atkinson, G., Boore, D., Bozorgnia, Y., Campbell, K., Chiou, B., Graves, R., Idriss, I.M., Stewart, J., Shantz, T. and Youngs, R. (2012). PEER NGA-West2 Database: A database of ground motions recorded in shallow crustal earthquakes in active tectonic regimes. *15th World Conference on Earthquake Engineering*. (Submitted).

Bommer, J. and Mendis, R. (2005). Scaling of spectral displacement ordinates with damping ratios. *Earthquake Engineering and Structural Dynamics*. **34**, 145-165.

Boore, D.M. (2010). Orientation-independent, non geometric-mean measures of seismic intensity from two horizontal components of motion. *Bulletin of the Seismological Society of America*. **100**, 1830-1835.

Boore, D.M., Watson-Lamprey, J. and Abrahamson, N.A. (2006). Orientation-independent measures of ground motion. *Bulletin of the Seismological Society of America*. **96**, 1502-1511.

Bozorgnia, Y. and Campbell, K.W. (2004). Engineering characterization of ground motion. Chapter 5 of Bozorgnia and Bertero (2004): "*Earthquake Engineering: From Engineering Seismology to Performance-Based Engineering*." CRC Press, Boca Raton, FL.

Cameron, W.I. and Green, I. (2007). Damping correction factors for horizontal ground-motion response spectra. *Bulletin of the Seismological Society of America*. **97**, 934-960.

Kempton, J.J. and Stewart, J.P. (2006). Prediction equations for significant duration of earthquake ground motions considering site and near-source effects. *Earthquake Spectra*. **22**, 985-1013.

Lin, Y.Y. and Chang, K.C. (2004). Effects of site classes on damping reduction factors. *Journal of Structural Engineering*, ASCE. **130**, 1667-1675.

Lin, Y.Y., Miranda, E. and Chang, K.C. (2005). Evaluation of damping reduction factors for estimating elastic response of structures with high damping. *Earthquake Engineering and Structural Dynamics*. **34**, 1427-1443.

McGuire, R.K., Silva, W.J. and Costantino, C.J. (2001). Technical basis for revision of regulatory guidance on design ground motions: Hazard- and risk-consistent ground motion spectra guidelines (Section 4.9: Estimation of spectra for other dampings). Report, NUREG/CR-6728. Prepared for Division of Engineering Technology, Office of Nuclear Regulatory Research, U.S. Nuclear Regulatory Commission, Washington, DC.

Naeim, F. and Kircher, C.A. (2001). On the damping adjustment factors for earthquake response spectra. *The Structural Design of Tall Buildings*. **10**, 361-369.

Newmark, N.M. and Hall, W.J. (1982). *Earthquake spectra and design*. Monograph, Earthquake Engineering Research Institute, Berkeley, CA.

PEER/ATC72-1 (2010): Pacific Earthquake Engineering Research Center / Applied Technology Council. *Modeling and acceptance criteria for seismic design and analysis of tall buildings*. Applied Technology Council, Redwood City, CA.

Power, M., Chiou, B., Abrahamson, N.A., Roblee, C., Bozorgnia, Y. and Shantz, T. (2008). An introduction to NGA. *Earthquake Spectra*. **24**, 3-21.

Regulatory Guide 1.61 Revision 1 (2007). Damping values for seismic design of nuclear power plants. U.S. Nuclear Regulatory Commission, Washington, DC.

Rezaeian, S., Bozorgnia, Y., Idriss, I.M., Campbell, K., Abrahamson, N. and Silva, W. (2012). *Spectral Damping Scaling Factors for Shallow Crustal Earthquakes in Active Tectonic Regions*, Pacific Earthquake Engineering Research Center, Berkeley, CA. (In Press).

Stafford, P.J., Mendis, R. and Bommer, J.J. (2008). Dependence of damping correction factors for response spectra on duration and numbers of cycles. *Journal of Structural Engineering*, ASCE. **134**, 1364-1373.

TBI (2010): Tall Buildings Initiative. *Guidelines for Performance-Based Seismic Design of Tall Buildings*. PEER Report 2010/05, November 2010. Prepared by the TBI Guidelines Working Group. Berkeley, California: Pacific Earthquake Engineering Research Center, University of California.